EXPERIMENTS WITH A VACUUM SPARK ION SOURCE

EXPERIMENTS WITH A VACUUM SPARK ION SOURCE

By

BISWESWAR CHAKRAVARTY, M.Sc.

A Thesis
Submitted to the Faculty of Graduate Studies
in Partial Fulfilment of the Requirements
for the Degree
Doctor of Philosophy

McMaster University

May 1963

DOCTOR OF PHILOSOPHY (1963)
(Physics)

McMASTER UNIVERSITY
Hamilton, Ontario

TITLE: Experiments with a Vacuum Spark Ion Source

AUTHOR: Bisweswar Chakravarty, B.Sc. (Hons.) (Dacca University)
M.Sc. (Dacca University)

SUPERVISOR: Professor H. E. Duckworth

NUMBER OF PAGES: vii, 59

SCOPE AND CONTENTS:

The principal aim of the present investigation is to extend our knowledge of the merits and demerits of the mass spectroscopic method of solid analysis. This dissertation provides information concerning relative ionization efficiencies for several elements and factors which effect these efficiencies. Secondary purposes of this work are 1) to make an independent determination of the temperature of the vacuum spark, 2) to resolve the current discrepancy concerning the value of the C_3^+/C_2^+ ratio from graphite electrodes in a spark and, finally, 3) to provide an accurate value for the Ni^{58}/Ni^{60} abundance ratio.

ACKNOWLEDGEMENTS

I am greatly indebted to my supervisor, Professor H. E. Duckworth, for his continuous guidance, encouragement, interest and advice throughout the course of this investigation. I also thank Dr. M. W. Johns and Dr. R. P. Graham for the advice rendered by them as members of my Supervisory Committee.

Much valuable assistance in the experimental work was given by Dr. V. S. Venkatasubramanian and Mr. Paul Van Rookhuyzen. My thanks are also due to Mr. Basil Wall for his help in calculations and to Mr. Tom Bryden and his staff for their technical help. I wish to express my thanks to the following for providing samples used in this work:

1. Greening Wire Company (Messrs. Duncan and Ledger)
2. Anaconda American Brass Co. (Mr. J. McCrackan)
3. Aluminium Laboratories Ltd. (Dr. R. H. Hay)
4. Dr. J. S. Kirkaldy and Mr. R. J. Brigham for $CuAl_2$ alloy.

Finally, my thanks are to Miss Heather Edmonstone for typing this thesis.

TABLE OF CONTENTS

LIST OF FIGURES

LIST OF TABLES

INTRODUCTION

The principal aim of the present investigation is to extend our knowledge of the merits and demerits of the mass spectroscopic method of solid analysis. The analysis of solids by mass spectroscopic methods possesses certain potential advantages over chemical and spectrochemical methods of analysis. On the one hand, chemical separations are avoided while, on the other, mass spectra are considerably less complicated than the corresponding optical spectra.

One of the main problems facing the mass spectroscopic method is that of obtaining a suitable source of ions. A well-behaved source such as the thermal ionization type is highly selective in action, and the same comment holds, to a lesser extent, for the oven type of source. The vacuum spark source, however, which was first introduced into mass spectroscopy by Dempster (1936), shows relatively little discrimination. The main drawbacks with this source are the following:

a) The ions from the source possess a wide energy spread ($\sim$1000 V), so that a double-focusing mass spectrometer is required.

b) The spark is subject to fluctuations in intensity, and produces considerable RF noise, so that electrical detection is not easy.

Some preliminary work on this problem of solid analysis was done by Dempster (1946), using a spark source and photographic detection. This work was considerably extended by Hipple and Gorman (1951), and Gorman, Jones and Hipple (1951), who employed an electrical, rather than a photographic,method of detection. By monitoring a representative fraction of the ion current entering the magnetic analyser, and recording the ratio of the resolved ion current to the monitor current, they were able to overcome the problem of the source intensity, and to carry out the analysis of major elements in steels. The photographic method was further developed by Hannay and Ahearn (1954), whose subject of study was trace impurities in semi-conductors. Recently, Craig, Errock and Waldron (1959) have pushed the matter further by developing a commercial double-focusing instrument intended for the analysis of impurities in solids. The sensitivity of this instrument is high, and semi-quantitative data can be obtained by comparing line densities on a series of mass spectra. The exposure for each of these mass spectra is known from the integrated monitor current, measured at the entrance to the magnetic analyser.

While the previous work (1951,1959) has shown that the relative ionization efficiencies in a spark source are of the same order of magnitude for all elements studied, and has provided relative ionization efficiency values for several elements as well, it is important to have more information of this sort. In the present work a system of electrical detection has been used to check certain existing relative ionization efficiency data and, in addition, to obtain some new data of a similar type.

In addition to the principal aim, as outlined above, the investigation has had certain specific secondary aims. The first of these is to make an independent estimate of the temperature of the vacuum spark, which can be compared to two corresponding, but conflicting, estimates made recently in Russia on the basis of studies of high-order spectra. The second is to resolve a current disagreement concerning the relative numbers of C_2 and C_3 aggregates produced in a vacuum spark. The third, and final, of these specific aims is to provide an accurate value for the Ni^{58}/Ni^{60} abundance ratio and, in passing, for the Cu^{63}/Cu^{65} abundance ratio. The former is desirable on grounds of precision, and both are desirable to ensure that previous determinations were not invalidated in part by fractionation of the isotopes. Any mass discrimination in the spark source would be negligible compared to other types of ion source.

CHAPTER I: APPARATUS AND EXPERIMENTAL PROCEDURE

The Instrument

The double-focusing mass spectrograph described by Duckworth (1950) (employed originally for mass measurements) has been used in the present work. This instrument was rebuilt during 1959 and certain modifications were made at that time. Among other things, an adjustable exit slit was introduced, followed by a Faraday Cup, in order to record the mass spectra electrically.

The instrument, which is shown schematically in Fig. 1, is of the Dempster (1935) design, in which a 90° radial electrostatic analyzer is followed by a 180° magnetic analyzer. The electrostatic analyzer has a mean radius of 7.9 inches, and is used asymmetrically with object and image distances $\ell_e' = 0.150\ a_e$ and $\ell_e'' = 0.609\ a_e$, respectively. The image formed by this analyzer is located at the effective boundary of the magnetic field so that the final image is formed at the exit boundary of the same ($a_m = 1.15\ a_e$). The dispersion of the instrument is 2.3 mm for 1% mass difference. While the instrument is capable of high resolving power (~ 7000 with a 0.001-inch principal slit and photographic detection), it has been operated, for the present work, with wide entrance and exit slits so as to yield a resolving power of the order of 60 - 100.

Vacuum System

The source and the analyzer regions are pumped separately with oil diffusion pumps backed by mechanical pumps. With prolonged pumping the pressure in each region can be reduced to about 10^{-6} mm of Hg. In a

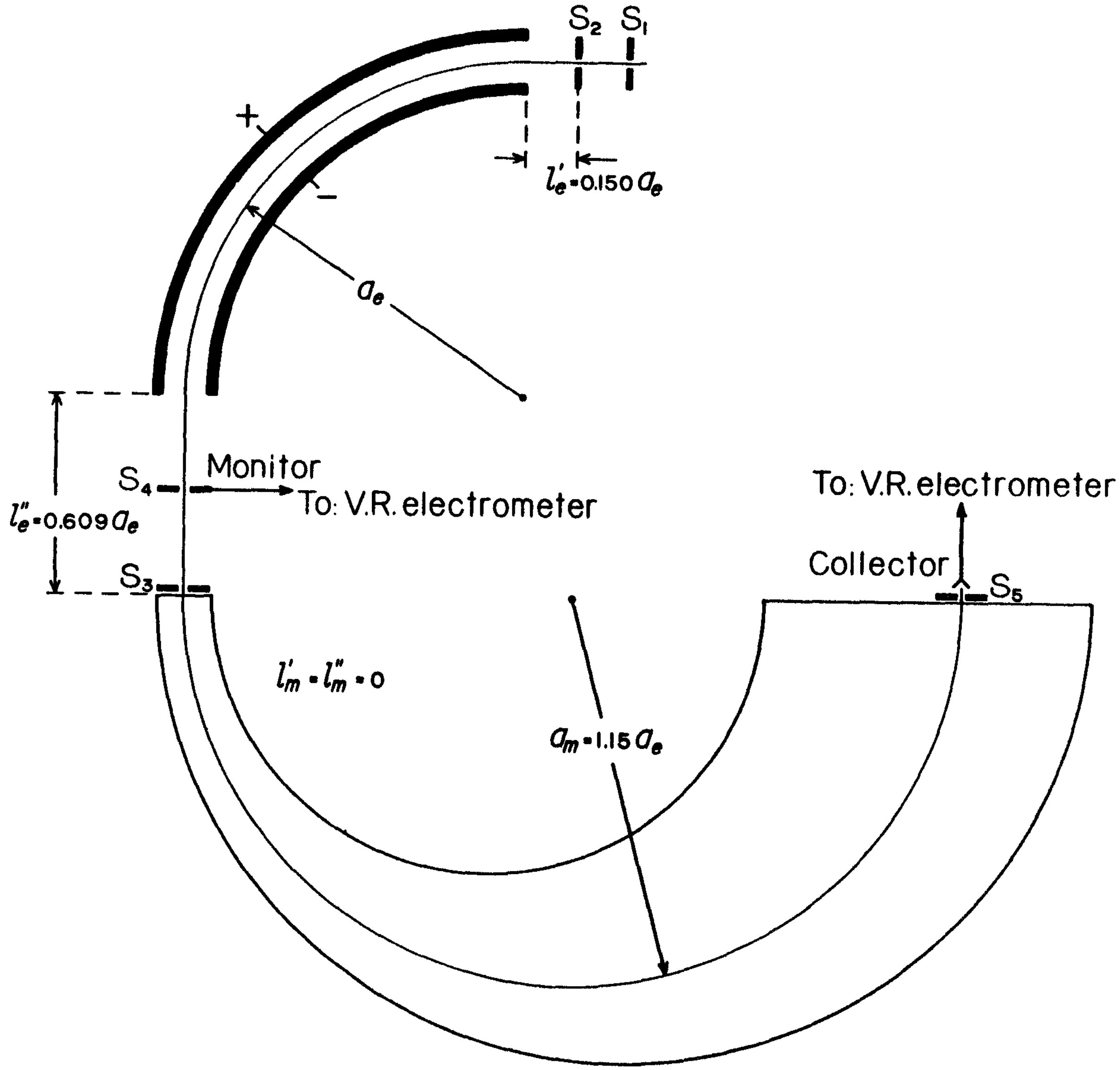

Figure 1

Schematic Diagram of the Mass Spectrometer reasonable time of a few hours, a pressure in the analyzer of 5×10^{-6} mm, and in the source region of 10^{-5} mm, can be reached. If the instrument were to be used for routine analysis, it would be desirable to add a vacuum lock between the source and the analyzer. This would make it possible to change electrodes without destroying the vacuum in the greater part of the apparatus.

Accelerating Voltage Supply (V_a)

This voltage supply is the same as in the original reference (Duckworth, 1950) except that a constant voltage transformer was introduced between the line and the power supply. This was necessary for the operation of an electron impact ion source which was used to align the instrument. This power supply provides up to 20 kV of half-wave rectified D.C., filtered with a 40-megohm resistor shunted by 2.25 microfarads of capacity. Thus, the time constant is $40 \times 10^{6} \times 2.25 \times 10^{-6} = 90$ sec. A 10-megohm protective resistor is provided for safety in series with the high voltage outlet.

Voltage Supply for the Electrostatic Analyzer (V_b)

The voltage across the electrostatic analyzer is supplied by a bank of batteries contained in a metal box which is provided with a lid. There are fifteen batteries (M2 type) in series, each of 45 volts. The connection to the condenser plates is made through Kovar-metal seals and spring connections. It was found that the intensity of the resolved ion beam is sharpest when the negative terminal is grounded. It was found necessary to shield completely the batteries and the leads to the electrostatic analyzer from the Tesla radiation. For optimum operation it was found experimentally

$$\frac{V_a}{V_b} \backsim 22.$$

Magnet Current Supply

The magnet current supply used in this work is not the same as that described in the original reference, which was designed with photographic detection in mind. For electrical recording of the ions it was necessary to build a stabilized magnet current supply which would permit a scanning of the ion beam. The magnet current supply that was constructed is very similar in design to that described by Thode et al (1947). The circuit diagram of this supply is given in Fig. 2. The current can be varied continuouslyfrom 11 to 130 mA. The scanning is usually done automatically, in which case the helipot R_{15} is driven by a motor whose speed can be controlled. The scanning can also be done manually.

The Spark Ion Source

The ion source used in this work is essentially of the type described in the original reference, viz. the spark takes place between a rod electrode of the material to be analyzed and the walls of a hole in a conducting disc. In this work the disc material was either tantalum or carbon. Provision was made for fine movement of the rod electrode. A diagram of the source arrangement is given in Fig. 3. Sample materials are handled in the form of rods 0.03 to 0.06 inches in diameter and 0.15 to 0.75 inches long. In the case of very brittle and very small samples, the sample is introduced in a nickel tubing with about 0.015 inches of the sample protruding. These rods are held by a pin vise. Since the tip of the rod sparks against the wall of the hole, the cross-sectional shape of the rod is not important. The spark is energized by a Tesla oscillator, the circuit diagram of which is given in Fig. 11 (Chapter II). The spark is pulsed 120 times per second and, while oscillating, has a frequency of about 4 megacycles.

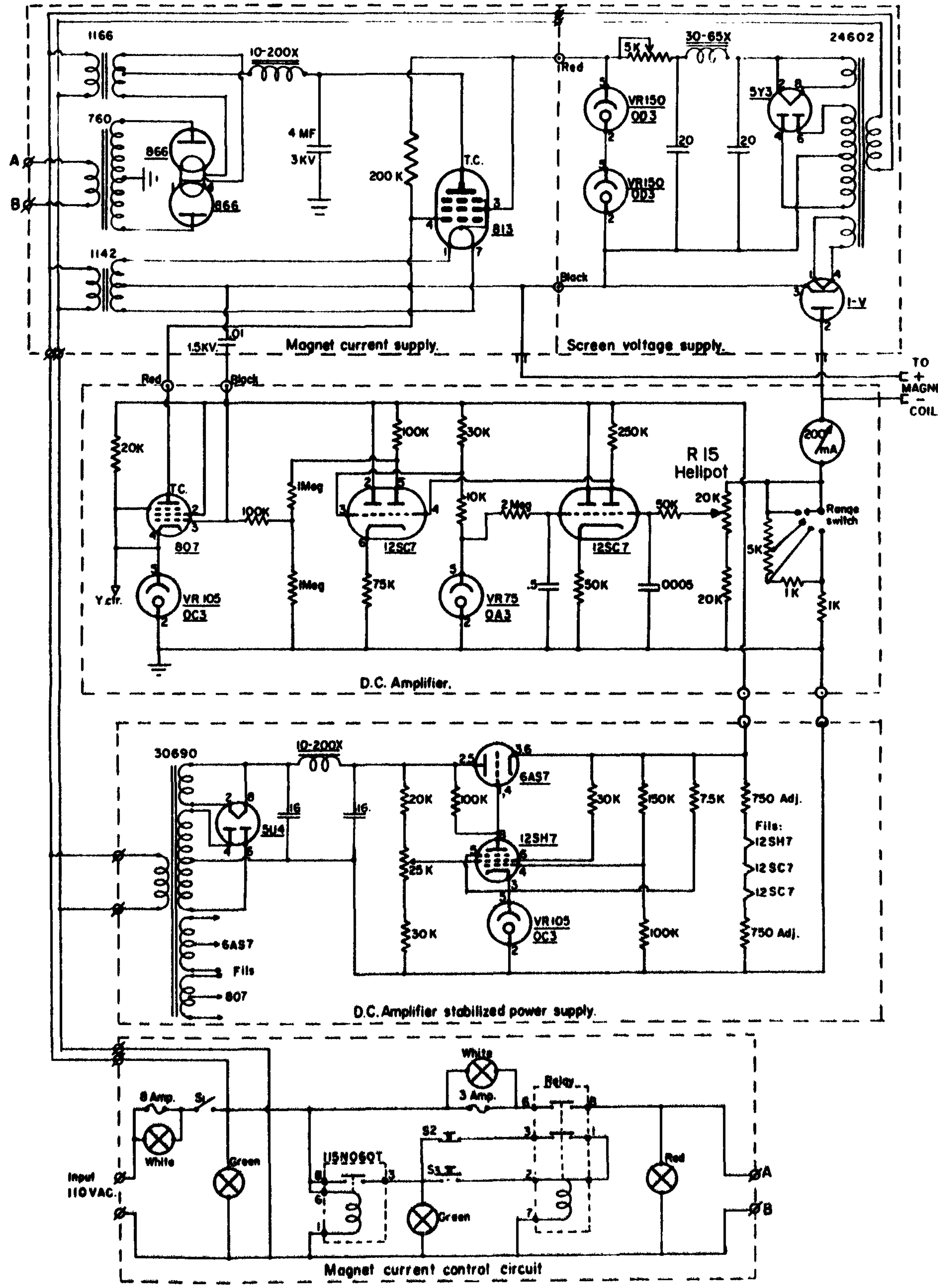

Figure 2

Magnet Current Supply

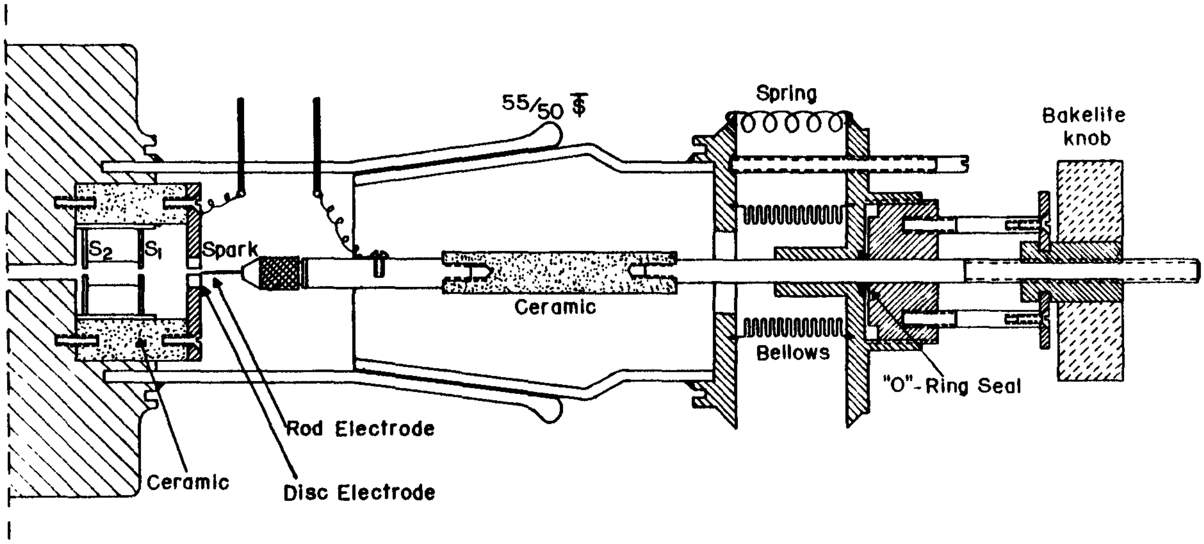

Figure 3

Schematic Diagram of the Source

Detection of Ions

The two well-known methods for detecting a beam of ions in a mass spectroscope are photographic detection and electrical detection. Hannay (1954), one of several who had used photographic detection in the mass spectroscopic analysis of solids, summarizes its merits as follows:

> "Photographic detection provides high sensitivity, integration of current despite source fluctuations and the simultaneous recording of a wide mass-range, but it is less quantitative, requires the introduction of the photographic plates into the vacuum system, and does not provide visual information while the source is in operation.".

Some of the difficulties in doing quantitative work arise from uncertainties in the blackening law of the plate, with respect to exposure, ion energy and ion mass. These difficulties can be avoided with a properly designed system of electrical detection. Electrical detection of ions, though desirable, is difficult in the case of a high vacuum spark because of the two main reasons mentioned in the Introduction, viz. a) wild fluctuations of the beam intensity and b) the large RF noise associated with the spark. One way to overcome the ion current fluctuations is to monitor the ion beam after energy selection and to measure the ratio of the resolved ion current to that of the monitor. Since the monitor represents the fluctuations of the beam current at any instant, then the ratio of the resolved ion current to that of the monitor is independent of source intensity fluctuations. Hipple, Gorman and Jones (1951) were the first to adopt this device and they demonstrated the potentiality of the method by carrying out an analysis of the major elements present in a stainless steel.

The same general method employed by Hipple <u>et al</u> (1951) has been employed in the present investigation. A monitoring slit (S_4 in Fig. 1) intercepts the peripheral portions of the beam transmitted by the electrostatic analyzer. The current reaching this monitor and the current arriving at the final collector are measured by two vibrating-reed electrometers. An adjustable slit (S_5 in Fig. 1) precedes the final collector. In order to measure the output voltages of the two electrometers, two identical recorders have been employed. The ratio of the two output voltages can easily be computed from the chart readings.

The final collector was simply an inverted "V" with both sides closed. No precautions were taken to suppress secondary electrons, inasmuch as the collector was in a strong fringing field, which provided automatic suppression.

The important question of RF noise and its shielding is discussed later under "Noise".

Experimental

The preliminary experiments were carried out with a brass sample (70% copper, 30% zinc) sparking against the walls of a hole in the tantalum disc. The alignment obtained with the electron impact ion source was kept practically undisturbed. The monitor slit was first withdrawn from the path of the beam and the magnetic field was scanned for resolved ion peaks. This step was taken so as not to miss the peaks that may be submerged in the not too favourable signal to noise ratio that prevails with the spark. When a peak was once obtained, the accelerating voltage (~15 kV) was adjusted for maximum reading. Then the monitor electrode was pushed in and adjusted for minimum monitor and maximum exit slit currents. The exit slit width was then gradually decreased until, by scanning the magnetic field, the resolved ion peaks (e.g. Cu^{63}, Zn^{64}, Cu^{65}, Zn^{66}, *et cetera*) could be recorded on the recorder chart. This same procedure was followed for the other material as well.

Monitor currents ranged from 10^{-10} A to 5×10^{-10} A, while the isotopic currents ranged from 10^{-11} A to 5×10^{-12} A. For certain experiments the monitor current was as large as 10^{-9} A. Some mass spectra obtained during various stages of operation are shown in Figs. 5 to 10.

Discussion on Noise

As a first step to reduce noise arising from the RF radiation from the spark the Tesla oscillator was heavily shielded, likewise the high voltage supply, source, condenser batteries and connecting cables. All the earth connections were grounded to the same water pipe to prevent earth-loop pick-up voltages. Special precautions were taken to prevent corona discharges. Occurrence of corona discharge in the neighbourhood of the source was always indicated by an increase in the noise level at the final collector. The method of suppressing noise reported by C. F. Robinson (1960), by providing an extra spark gap (in a hermitically sealed glass tube provided with two electrodes) in the path of one of the sparking electrodes, was tried without much success. A low resistance (wire-wound) in the path was also of no advantage.

A few other ways in which the noise level was reduced are now described.

a) A significant reduction in noise was achieved by insertion of a series resistance in the input circuit to the vibrating-reed electrometers, as shown in the accompanying diagram.

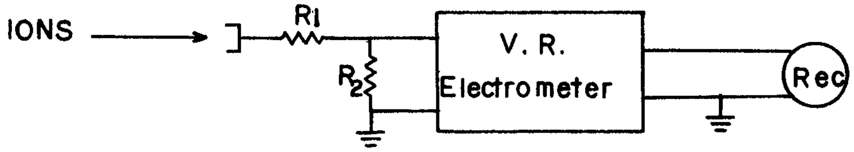

Fig.4

R_1 has the value 10^{10} ohms and R_2 has the value of 10^{11} ohms. This circuit behaves essentially as an integrating circuit.

b) The violent spark with much visible light output is always found to be associated with large noise. The spark has been found to be most efficient in producing ions when the spark is steady and quiet, and under this condition the noise is also the lowest. The most suitable spark on all counts is when the rod electrode is very close to the hole in the disc and symmetrical with respect to the hole and sparking takes place between the walls of the hole and tip of the rod.

c) With long continued sparking the noise always increases with time. This is at least partially associated with micro-discharges inside the source, caused by the deposition of vaporized metals on the inner walls of the source housing, where they provide conducting paths. A well-cleaned source housing, with fresh electrodes, has always lowered the noise level.

d) Noise seems to be larger with certain metals as electrodes than with others. For example, in the case of the tantalum disc electrode, the noise is always lower with the metals zinc, copper and silver; whereas, it is always higher with nickel, molybdenum and steel. There was a remarkable reduction in noise when the tantalum disc, which was first used, was replaced by a carbon disc. There are additional advantages in using a carbon disc, viz. carbon can be obtained in a very pure state, is easy to machine and is much less expensive than tantalum.

#712A ANALYSIS

SINGLY and DOUBLY CHARGED SPECTRA

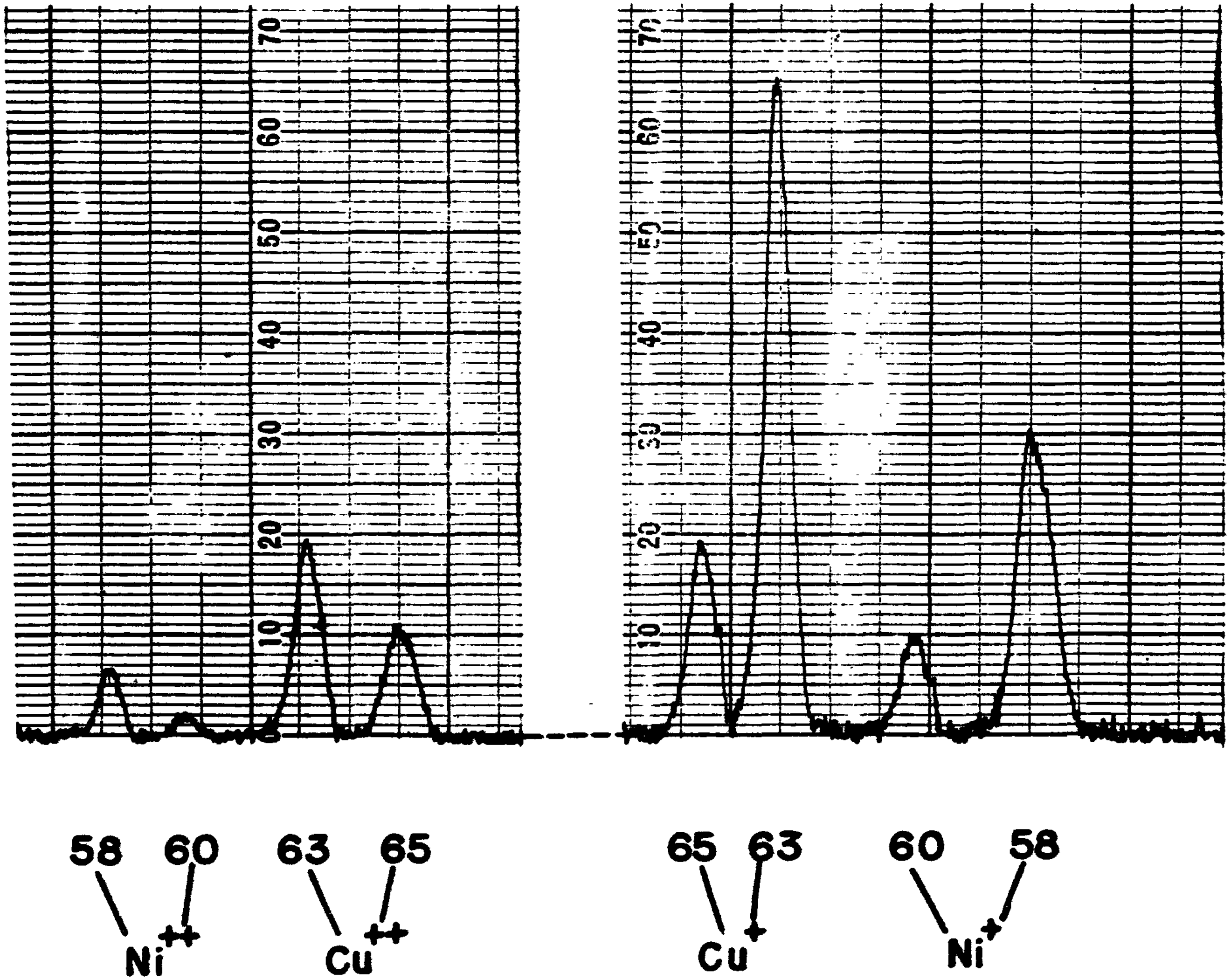

Fig. 5

#755 ANALYSIS

SINGLY and DOUBLY CHARGED SPECTRA

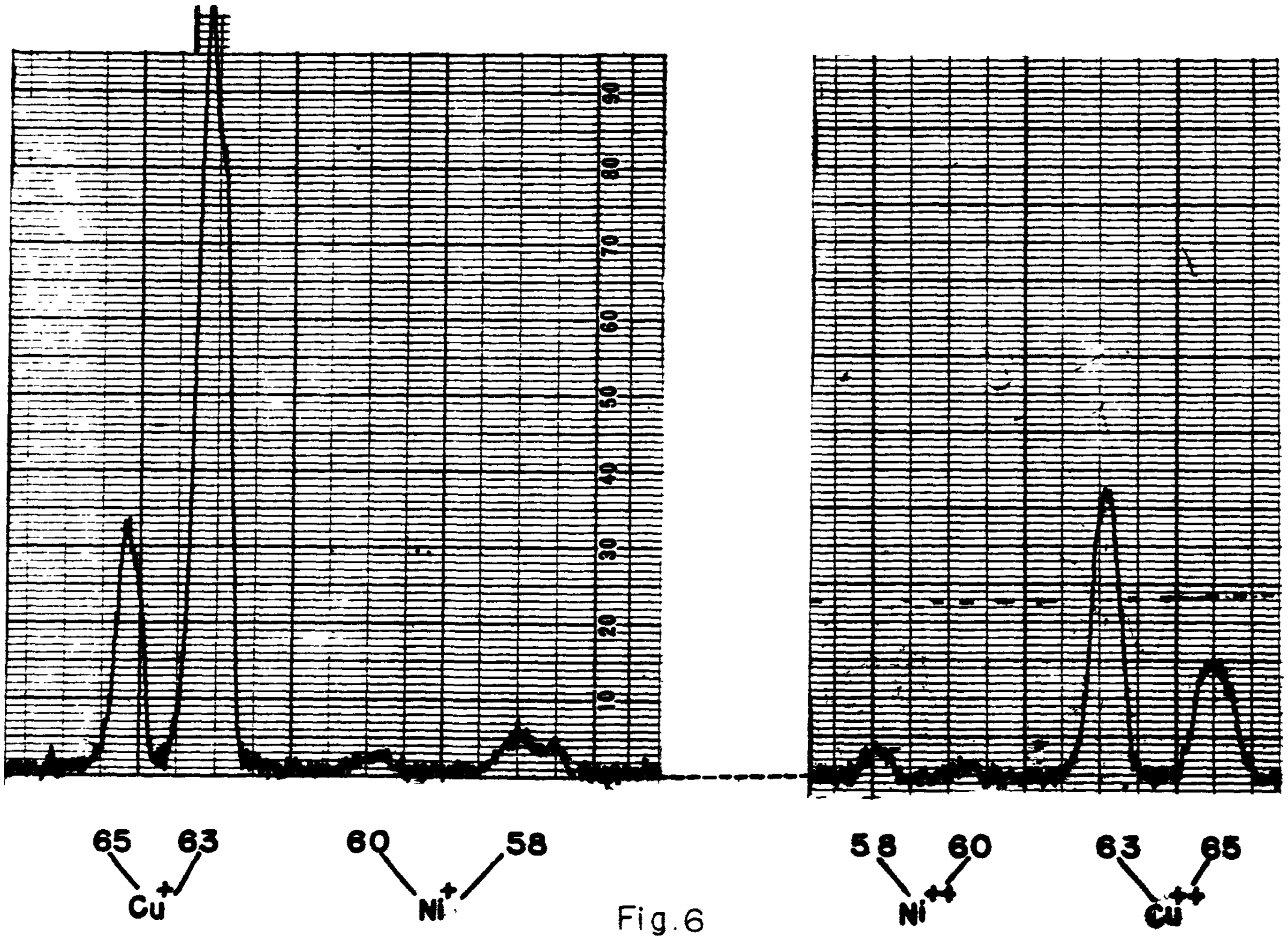

Fig. 6

#702RB ANALYSIS

SINGLY and DOUBLY CHARGED SPECTRA

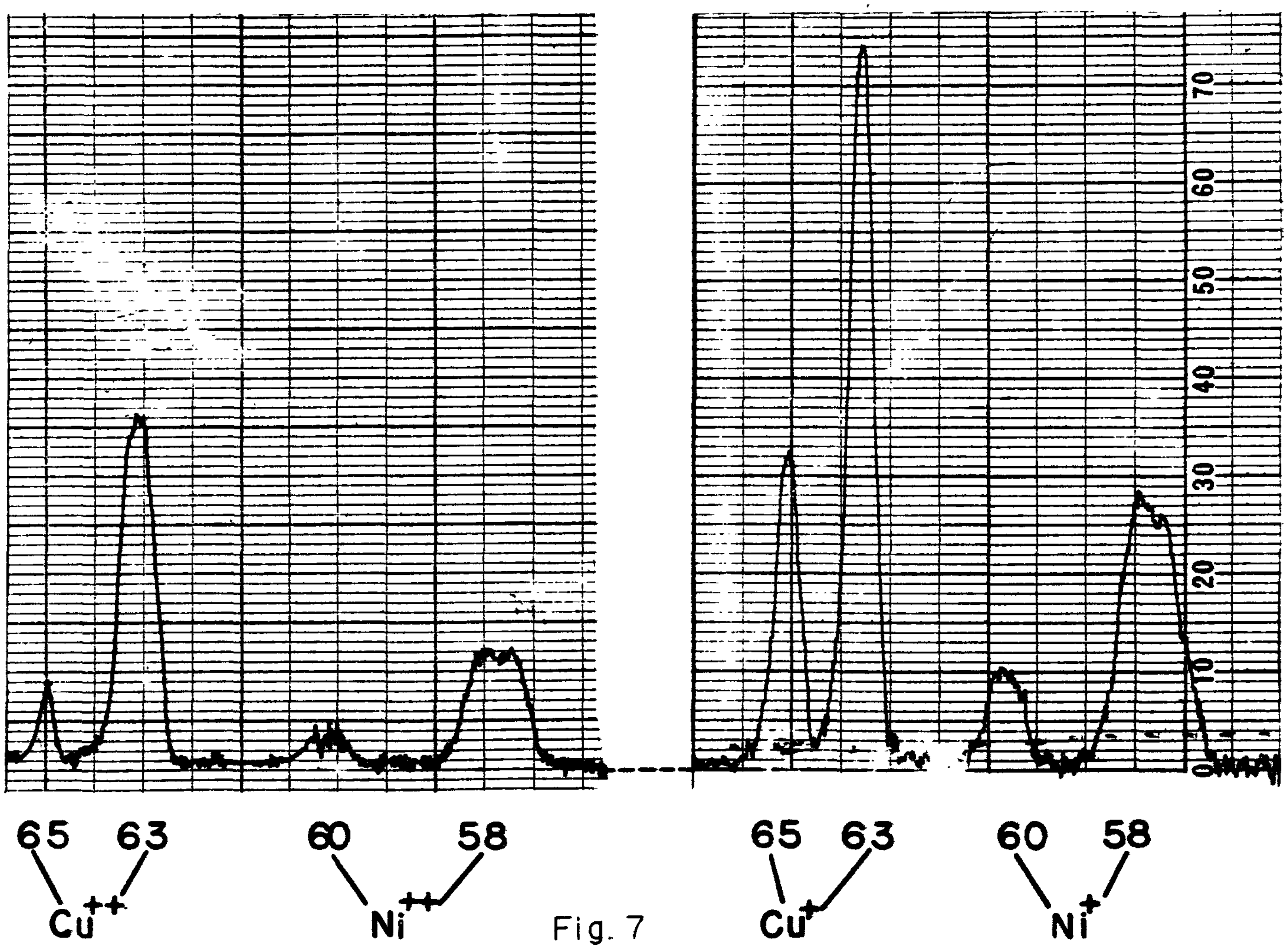

Fig. 7

#017 ANALYSIS

SINGLY, DOUBLY and TRIPLY CHARGED SPECTRA

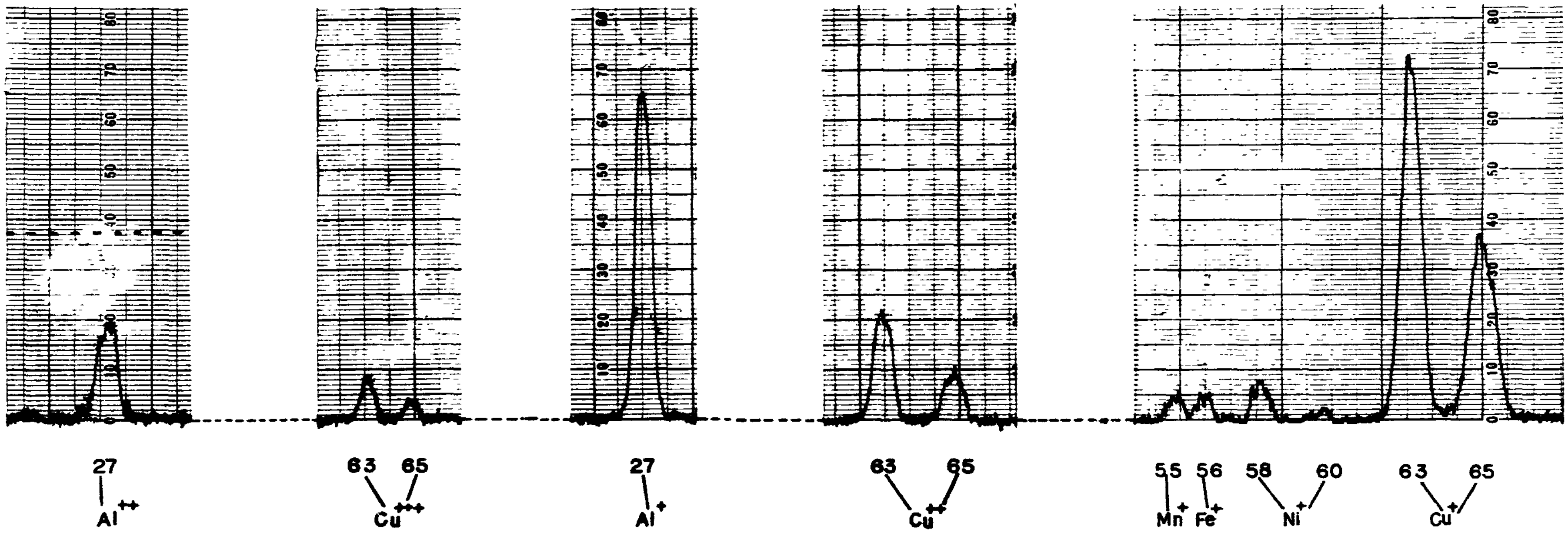

Fig. 8

COPPER ANALYSIS

SINGLY, DOUBLY and TRIPLY CHARGED SPECTRA

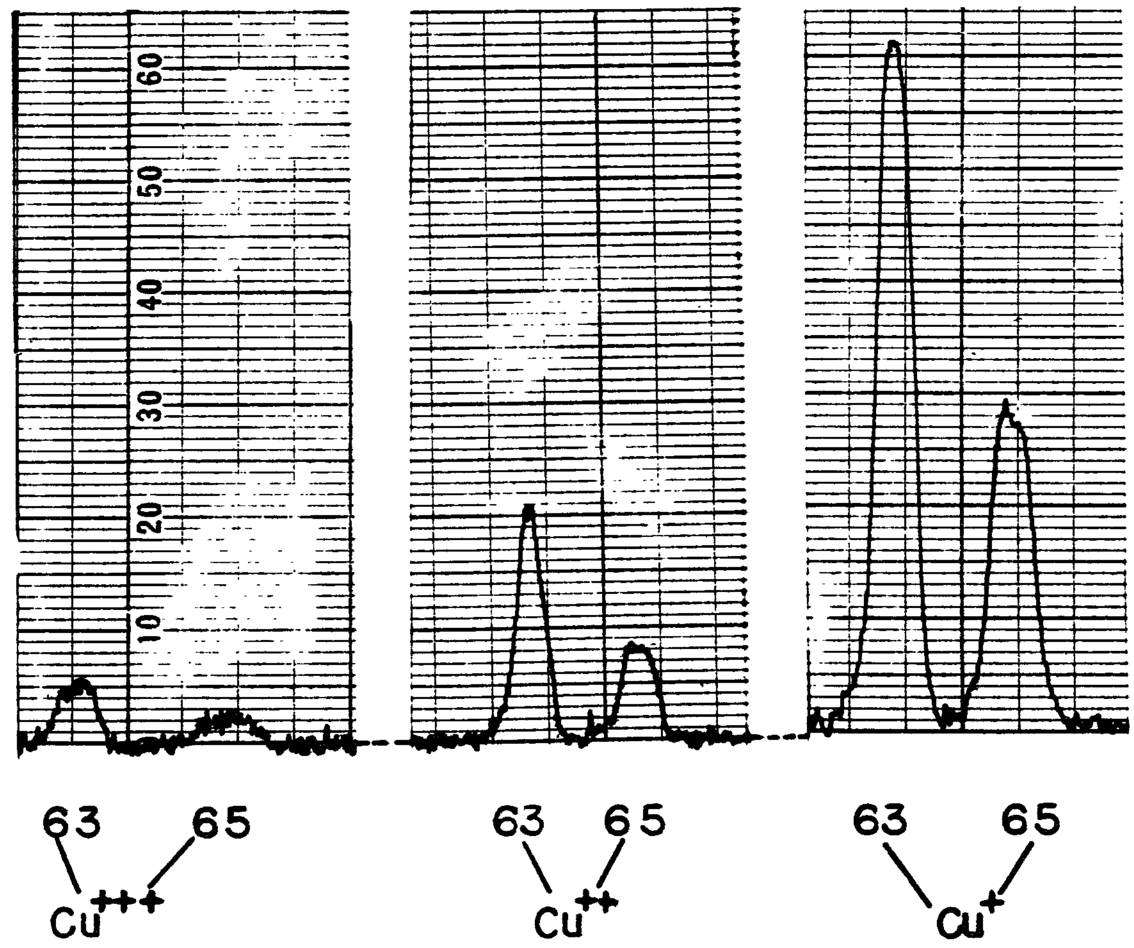

Fig. 9

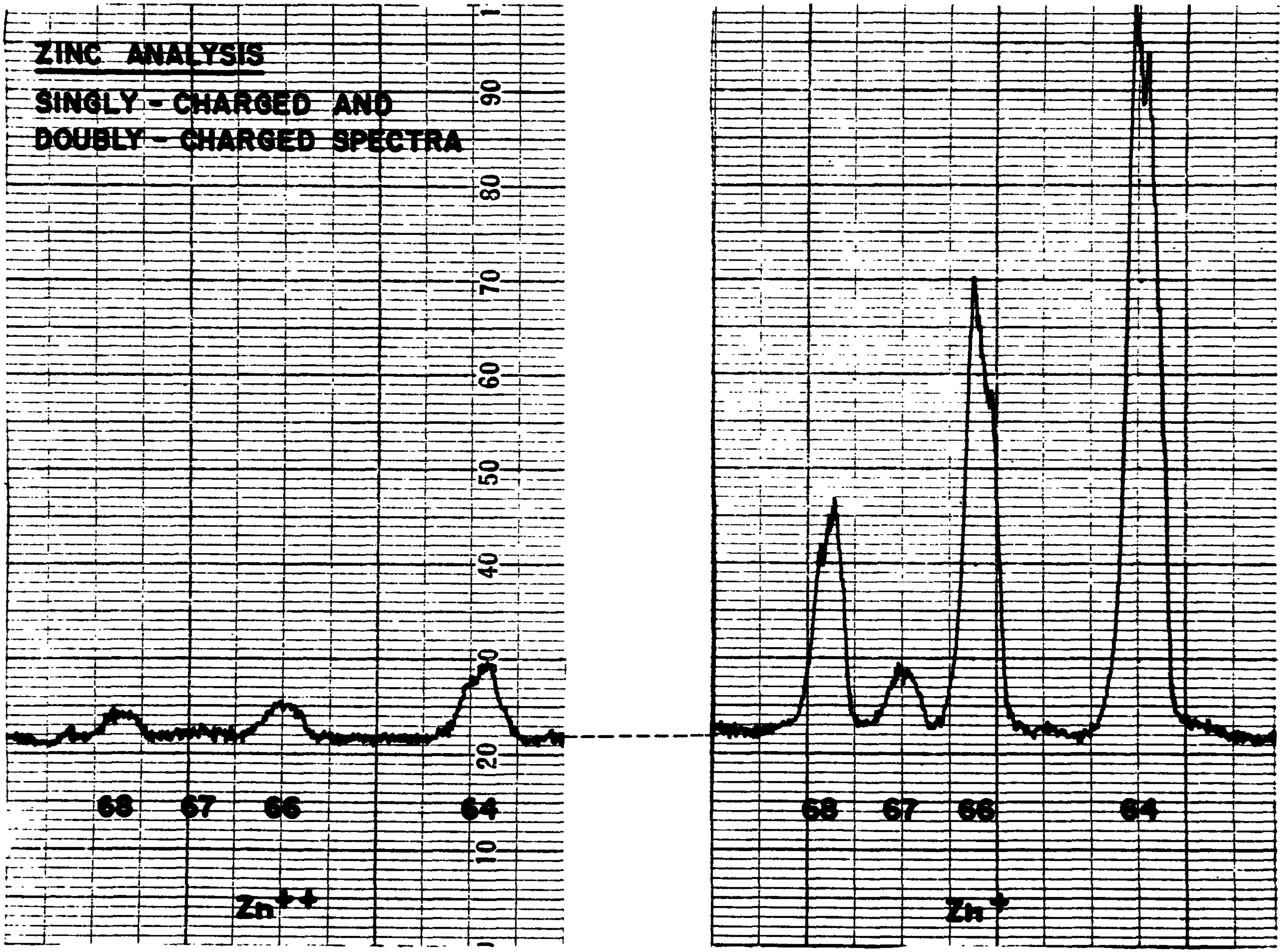
ZINC ANALYSIS
SINGLY - CHARGED AND
DOUBLY - CHARGED SPECTRA
90
80
70
60
50
40
30
20
10
68
67
66
64
Zn++
68
67
66
64
Zn+

Fig. 10

CHAPTER II: RELATIVE IONIZATION EFFICIENCIES FOR ELEMENTS IN A HIGH FREQUENCY SPARK ION SOURCE

A brief summary of the development of the mass spectroscopic analysis of solids using a vacuum spark ion source has been given in the Introduction. We shall now proceed to describe new results that bear on this subject.

Ionization Efficiency Calculations

The definition of ionization efficiency and the method of its calculation are illustrated by an example. Suppose a sample consists of two elements A and B and is analyzed with a mass spectrometer, yielding the resolved peak heights x and y, respectively. The elements A and B are conveniently chosen to be anisotopic. The relative ionization efficiency (that is, of A relative to B) is given by

$$\text{Relative ionization efficiency} = \frac{x/\text{number of atoms of A present in sample}}{y/\text{number of atoms of B present in sample}}$$

In the present experiment x is actually the ratio of the resolved ion peak of A to that of the monitor, and y is similarly the ratio of the resolved ion peak of B to that of the monitor. If A and B are isotopic, which is usually the case, then the relative ionization efficiences of the various isotopes are calculated, considering their abundances, in a manner that is described below. The efficiencies for the isotopes of the same element are essentially constant. The average efficiency of the isotopes of one element is then compared with the average efficiency of the isotopes of the other element. Using many samples in such a way that each adjacent pair has at least one element in common, an intercomparison of relative ionization efficiencies of several elements is possible. These may then be expressed relative to that element in the group (here nickel) which ionizes least efficiently in the spark. A tabulation of such values is given later (Table II).

Sample Calculation: Let us consider an alloy of nickel and copper, No.712A (Anaconda American Brass Co.), having the composition copper 77.24%, nickel 21.71%, iron 0.54%, manganese 0.51%, zinc $< 0.10\%$. Here the atoms of copper and nickel are in the ratio (77.24/63.54)/(21.71/58.71), where 63.54 and 58.71 are the atomic weights of copper and nickel respectively. Let S be the amount of sample burnt and ϵ_1 and ϵ_2 the respective absolute ionization efficiencies of copper and nickel. We have isotopic abundances $Cu^{63} = 69.1\%$, $Cu^{65} = 30.9\%$ and $Ni^{58} = 67.76\%$, $Ni^{60} = 26.16\%$. Thus representative peak heights are given by

$$Cu^{65} \text{ peak} = K \frac{S \times 77.24 \times 30.9}{63.54} \times \epsilon_1 \qquad (2\text{-}1)$$

$$Ni^{58} \text{ peak} = K \frac{S \times 21.71 \times 67.76}{58.71} \times \epsilon_2 \qquad (2\text{-}2)$$

where K, the proportionality constant, includes the transmission of the mass spectrometer. K is assumed to be the same for both ion groups, a reasonable assumption inasmuch as both groups travel identical paths to the collector.

For simplicity we refer to 'peak heights', but it is understood everywhere that resolved peak heights are divided by the corresponding monitor current. It is the ratio of the two that appears in the calculation. From (2-1) and (2-2), the ionization efficiency of copper relative to nickel is given by,

$$\frac{\epsilon_1}{\epsilon_2} = \left[\frac{Cu^{65}\text{ peak}}{Ni^{58}\text{ peak}}\right] \times \left[\left(\frac{67.76}{30.9}\right) \times \left(\frac{63.54}{58.71}\right) \times \left(\frac{21.71}{77.24}\right)\right] \tag{2-3}$$

or, written in full

$$\frac{\epsilon_1}{\epsilon_2} = \frac{\left[\frac{Cu^{65}\text{ peak}}{\text{corresponding monitor}}\right]}{\left[\frac{Ni^{58}\text{ peak}}{\text{corresponding monitor}}\right]} \times f_1$$

where

$$f_1 = \left(\frac{67.76}{30.9}\right) \times \left(\frac{63.54}{58.71}\right) \times \left(\frac{21.71}{77.24}\right) = 0.667$$

We now do the same for other combinations of isotopes.

$$\frac{\epsilon_1}{\epsilon_2} = \left[\frac{Cu^{63}\text{ peak/monitor}}{Ni^{58}\text{ peak/monitor}}\right] \times f_2 \quad \text{where} \quad f_2 = \left(\frac{67.76}{69.1}\right) \times \left(\frac{63.54}{58.71}\right) \times \left(\frac{21.71}{77.24}\right) = 0.298$$

$$\frac{\epsilon_1}{\epsilon_2} = \left[\frac{Cu^{65}\text{ peak/monitor}}{Ni^{60}\text{ peak/monitor}}\right] \times f_3 \quad \text{where} \quad f_3 = \left(\frac{26.16}{30.9}\right) \times \left(\frac{63.54}{58.71}\right) \times \left(\frac{21.71}{77.24}\right) = 0.258$$

$$\frac{\epsilon_1}{\epsilon_2} = \left[\frac{Cu^{63}\text{ peak/monitor}}{Ni^{60}\text{ peak/monitor}}\right] \times f_4 \quad \text{where} \quad f_4 = \left(\frac{26.16}{69.1}\right) \times \left(\frac{63.54}{58.71}\right) \times \left(\frac{21.71}{77.24}\right) = 0.115$$

The four efficiency ratios thus obtained are then averaged to obtain a single value for that run. A typical tabulation is shown in Table I.

Preliminary Survey

In order to identify certain problems that warranted detailed investigation, experiments were done to obtain approximate values for the relative ionization efficiencies of a number of representative elements. Samples of commercially-available alloys of known composition and an alloy of the intermetallic compound $CuAl_2$ were examined in this work, using

TABLE I: Typical Data for Calculating $\epsilon^+ = Cu^+/Ni^+$

Isotope	Peak Height P	Monitor M	Ratio (P/M)	$\epsilon = \epsilon_1/\epsilon_2$	
Cu^{65}	8	13	0.615	Cu^{65}/Ni^{58}	1.26
Cu^{63}	26	21	1.24	Cu^{63}/Ni^{58}	1.14
Ni^{60}	3.5	28	0.125	Cu^{65}/Ni^{60}	1.27
Ni^{58}	7.5	23	0.325	Cu^{63}/Ni^{60}	1.14

Average $\epsilon^+(Cu^+/Ni^+)$ for the run = 1.20

tantalum as the disc electrode. The results of these experiments are shown in Table II, where they are compared to those obtained by Gorman, Jones and Hipple (1951) and Craig, Errock and Waldron (1959). The information in Table II was obtained from the analysis of the alloys shown in Table III.

It is seen from Table II that the relative ionization efficiencies of the elements examined in this work lie within a factor of 3 of one another. These results are in reasonable agreement with those given by Craig et al (1959) on the basis of photographic measurements, and also they agree well with those obtained by Gorman, Jones and Hipple (1951). It is found, with elements of high efficiency, such as zinc and magnesium, that there is a discrimination effect with long-continued sparking, the zinc and magnesium peaks increasing in intensity. This is probably to be attributed to deposition of the rod material on the tantalum disc electrode. The values given in Table II refer to the earliest sparkings.

While the mechanism of the vacuum spark discharge is imperfectly understood, it is generally assumed (Meek and Craggs, 1953) that a pure electron discharge is initiated by field emission. This vaporizes the anode surface by electron bombardment and gives rise to a cloud of vapour. Ionization of the latter then takes place by electron impact. Determinations of the temperature of a vacuum spark (see Chapter III) suggest that it lies between 5×10^4 and 2×10^5 degrees Kelvin. The fact that the relative ionization efficiencies are of the same order of magnitude for the elements studied suggests that, at such high effective temperatures, there is no serious discrimination in either the vaporization or ionization processes. Indeed, it is believed that a high temperature plasma is formed and thermal equilibrium exists within it.

TABLE II: Relative Ionization Efficiencies of Singly-Charged Ions

Element	This Work	Gorman, Jones and Hipple (1951)	Craig, Errock and Waldron (1959)
Mg	2.9	-	-
Al	1.1	-	-
Si	-	-	1.8
Ti	-	-	1.2
Cr	1.7	1.68	-
Mn	2.5	-	2.0
Fe	1.2	1.12	1.1
Ni	1.0	1.0	1.0
Cu	1.25	-	0.9
Zn	2.3	-	6.1

TABLE III: Materials Analyzed to Compile Data in Table II

No.	Alloy	Composition
1	Brass	70% Cu, 30% Zn
2	Monel	60% Ni, 33% Cu, 7% Fe
3	Nichrome	60% Ni, 16% Cr, 24% Fe
4	Manganese Steel	85% Fe, 15% Mn
5	Magnalium	10% Mg, 90% Al
6	Intermetallic Compound $CuAl_2$	56% Cu, 44% Al
7	Nickel Silver	55% Cu, 18% Ni, 27% Zn
8	Chromel	35% Ni, 20% Cr, 45% Fe
9	Manganin	82% Cu, 15% Mn, 3% Ni

Some preliminary measurements were also carried out for some elements of the relative abundances, in the vacuum spark, of singly- and doubly-charged ions. In each case, a rod of the material was sparked against a disc of tantalum, and the abundance ratios of singly- to doubly-charged ions were computed as averages for the isotopes of each element. The results of these experiments are shown in Table IV.

These results are interesting as they indicate an influence of the electrode materials on the effective temperature of the spark. As can be seen from Table IV, a rod of pure copper gives a relatively higher abundance of the doubly-charged ions than does a rod of pure zinc. On the other hand, with a brass electrode (70% copper, 30% zinc), the abundance of Cu^{++} ions is significantly lower than with the pure copper electrode, whereas the abundance of Zn^{++} is approximately the same as before. The lower abundance of doubly-charged ions of zinc from the pure specimen, and of zinc and copper from brass, can presumably be attributed to a cooling of the spark column by the high rate of volatilisation of the zinc (B.P. 907°C compared to copper whose B.P. is 2336°C). Clearly the ionization efficiency for Cu^{++} ions is greatly altered in the presence of zinc and, presumably, it might be altered in the presence of certain other elements as well. This dependence of the ionization efficiency upon the environment has not been reported for singly-charged ions, but it must almost certainly exist, albeit to a lesser extent. It is an effect which, if it exists, could be of crucial importance to the accuracy of the mass spectroscopic analysis of solids.

Thus, the chief result of the preliminary survey, apart from the intrinsic use of the results obtained, was to suggest the importance

TABLE IV: Relative Abundances of Singly- and Doubly-Charged Ions

Sample	Ionic Species	Ratio of Currents	Abundance Ratio
Pure copper	Cu^+, Cu^{++}	4	8
Pure zinc	Zn^+, Zn^{++}	9.5	19
Brass 30% Zn 70% Cu	Cu^+, Cu^{++}	8.5	17
	Zn^+, Zn^{++}	8.8	17.6

$\frac{I^+}{I^{++}}$ is the ratio of currents

$\frac{N^+}{N^{++}}$ is the abundance ratio of investigating the effect of the environment upon relative ionization efficiences. The results of one such detailed investigation are described in the next section under the heading " Composition Effect" .

Composition Effect

With carbon as the disc electrode, four alloy samples (provided by Anaconda American Brass Co.), each containing nickel and copper in differing amounts as shown in Table V, were analyzed in the manner described above. Mass spectra containing both singly- and doubly-charged ions were obtained in sufficient number to yield accurate values for the relative ionization efficiencies. The results are summarized in Table V.

The three alloys 702RB, 712A and 755 have also been analyzed with a tantalum disc as one of the electrodes. The results are tabulated in Table VI.

It is seen in Table V that the first three samples, which are essentially copper-nickel alloys, display a small but significent composition or " matrix" effect. This is not evident in Table VI, where the data are not so accurate, but they do indicate that $\mathcal{E}^+$ does not change much in shifting from a tantalum to a carbon disc.

This composition effect is not unexpected on the basis of experience gained in optical spectroscopy, where relatively small variations in concentration are sometimes found to produce large changes in the light emitted by a given constituent. To the writer's knowledge, however, it has not been demonstrated previously that the relative ionization efficiency for a singly-charged ion is dependent upon its environment, although a discussion remark (Chakravarty <u>et al</u>, 1962) at the Oxford Conference on Mass Spectrometry indicates that it has been

TABLE V: Relative Ionization Efficiencies (Cu^+/Ni^+ and Cu^{++}/Ni^{++}) from Various Copper-Nickel Alloys

Sample	Composition		$\epsilon^+ = Cu^+/Ni^+$	$\epsilon^{++} = Cu^{++}/Ni^{++}$
No. 702RB	Cu	68.62%	1.23 ± 0.02	1.02 ± 0.03
	Ni	30.22%		
	Mn	0.56%		
	Fe	0.60%		
	Zn	< 0.10%		
No. 712A	Cu	77.24%	1.14 ± 0.02	1.06 ± 0.03
	Ni	21.71%		
	Fe	0.54%		
	Mn	0.51%		
	Zn	< 0.10%		
No. 755	Cu	88.26%	1.10 ± 0.02	0.97 ± 0.03
	Ni	9.79%		
	Fe	1.41%		
	Mn	0.54%		
	Zn	< 0.10%		
No. 917	Cu	82 %	1.15 ± 0.02	-
	Al	9.5 %		
	Ni	5 %		
	Fe	2.5 %		
	Mn	1 %		

TABLE VI: Relative Ionization Efficiences $\epsilon^+ = Cu^+/Ni^+$ from Various Copper-Nickel Alloys (with Tantalum Disc)

Sample	$\epsilon^+ = Cu^+/Ni^+$
No. 702RB	1.14 ± 0.05
No. 712A	1.16 ± 0.05
No. 755	1.06 ± 0.05

suspected. The result is especially important inasmuch as the three alloys chosen for this investigation are so similar in nature. Presumably, larger changes could be found among a less homogeneous group of alloys. The effect, however, would be hard to see with the precision used in the Preliminary Survey (Table II), and was in fact not observed. On the other hand, the relative ionization efficiency for doubly-charged ions appears to be constant for the alloys. Incidentally, no ionization efficiences for doubly-charged ions had been published prior to this work.

The fourth alloy shown in Table V possesses a good deal of aluminum, an element that was lacking in the other three alloys. Its presence apparently has the effect of reversing the trend to lower ϵ^+ values as the nickel content decreases. Thus, we have an additional example of the composition effect.

Using three of these alloys plus pure copper and nickel (all with a carbon disc), additional spectra were obtained to provide the information relating to relative numbers of singly- and doubly-charged ions which is summarized in Table VII.

A consistency test (for the alloys No. 702RB, No. 712A, and No. 755) between the data in Tables V and VII shows reasonably good agreement, as can be seen by the following.

Let $Cu^+/Ni^+ = a$ and $Cu^{++}/Ni^{++} = b$, where a and b are measured relative ionization efficiencies as given in Table V. Let $Cu^+/Cu^{++} = c$ and $Ni^+/Ni^{++} = d$, where c and d are measured abundance ratios (that is, relative ionization efficiencies) as given in Table VII.

TABLE VII: Singly- to Doubly-Charged Abundance Ratios (Cu^+/Cu^{++} and Ni^+/Ni^{++}) from Various Electrodes

Sample	Ionic Species	Current Ratios (+/++)	Abundance Ratios (+/++)
Pure copper	Cu^+, Cu^{++}	4.5 ± 0.4	9 ± 0.8
Pure nickel	Ni^+, Ni^{++}	4.4 ± 0.3	8.8 ± 0.6
No. 702RB	Cu^+, Cu^{++}	6.6 ± 0.5	13.2 ± 1.0
	Ni^+, Ni^{++}	5.6 ± 0.5	11.2 ± 1.0
No. 712A	Cu^+, Cu^{++}	6.9 ± 0.2	13.8 ± 0.4
	Ni^+, Ni^{++}	6.5 ± 0.2	13.0 ± 0.4
No. 755	Cu^+, Cu^{++}	7.1 ± 0.2	14.2 ± 0.4
	Ni^+, Ni^{++}	6.9 ± 0.3	13.8 ± 0.6

$$\therefore \frac{c}{d} = \frac{Cu^{+}/Cu^{++}}{Ni^{+}/Ni^{++}} = \frac{Cu^{+}}{Cu^{++}} \times \frac{Ni^{++}}{Ni^{+}} = \frac{Cu^{+}}{Ni^{+}} \times \frac{1}{Cu^{++}/Ni^{++}}$$

$$= \frac{a}{b}$$

Corresponding values of a/b and c/d are shown in Table VIII. The agreement is significant inasmuch as few of the same spectra were used to compile both Table V and Table VII.

TABLE VIII: Consistency Test for the Data of Table V and Table VII

Alloy	a/b	c/d
No. 702RB	1.21 ± 0.04	1.18 ± 0.10
No. 712A	1.08 ± 0.04	1.06 ± 0.05
No. 755	1.14 ± 0.05	1.03 ± 0.05

The results shown in Table VII suggest that the +/++ ratios from the pure metal are lower for both copper and nickel than they are from the three alloys. Although there is no obvious dependence upon the percentages of the elements present, the +/++ ratios shown in Table VII provide tentative additional evidence for the type of composition effect which was seen so clearly in the Preliminary Survey when copper ions were obtained a) from pure metal and b) from brass.

Alloy 917, which contained five major constituents, provided an unusual opportunity to compute simultaneously the relative ionization efficiencies for all of the elements in this group. Although the experiments described above make it clear that ionization efficiencies are not unique, but depend upon the environment, it is instructive to compare the results obtained for alloy 917 with those obtained for the same elements in the Preliminary Survey. Those latter, it will be recalled, were obtained from the analysis of a group of alloys such that two adjacent alloys had at least one element in common. The two sets of results also differ in that alloy 917 was sparked against a carbon disc, and the Preliminary Survey results were obtained with a tantalum disc. The disagreement in the case of aluminum probably reflects an erroneous preliminary value, which was based on few and poor spectra. Other differences, if any, are slight.

TABLE IX: Relative Ionization Efficiences, ϵ^+, for Singly-Charged Ions

Element	No. 917 (C)	Preliminary Survey (Ta)
Al	1.74 ± 0.2	1.1
Mn	2.69 ± 0.09	2.5
Fe	1.14 ± 0.03	1.2
Ni	1.0	1.0
Cu	1.14 ± 0.02	1.25

The abundances of certain multiply-charged ions relative to singly-charged ions were also observed for alloy 917. These values are compared in Table X with the corresponding results for pure metals.

TABLE X: Abundance Ratios (+/++ and +/+++) from Pure Copper, Pure Aluminum, and Alloy 917

Sample	Cu^+/Cu^{++}	Cu^+/Cu^{+++}	Al^+/Al^{++}
Pure Cu	9.0 ± 0.8	33 ± 5	-
Pure Al	-	-	7.8 ± 0.6
No. 917 alloy	11.4 ± 1.2	52 ± 7	6.8 ± 1.0

Although the +/++ abundance ratios for aluminum seem to be practically the same for both the pure element and for the alloy, the efficiency of production of multiply-charged ions of copper is distinctly poorer with the alloy than with the pure copper electrode. Although the effect is not as marked as the pure copper versus copper-in-brass effect in the preliminary survey, it is probably explicable in the same way (aluminum boiling point ~2000°C; copper boiling point ~2300°C).

Multiply-Charged Ions from Pure Elements

Abundance ratios of the ionic species for some pure elements have been measured. Table XI gives the results obtained with a carbon disc electrode, while Table XII gives some early, less accurate, values obtained with a tantalum disc.

It might have been thought desirable to make both disc and rod electrodes of the material under study. The use of carbon, however, greatly reduced the noise from the spark and, consequently, improved the precision. The fact that the boiling points of both carbon and tantalum

TABLE XI: Abundance Ratios of Ionic Species for Pure Elements (with Carbon Disc)

Element	N^+/N^{++}	N^+/N^{+++}
Zn	16.6 ± 1.2	
Cu	9.0 ± 0.8	33 ± 5
Ni	8.8 ± 0.6	
Co	12.8 ± 1.2	
Fe	7.8 ± 0.6	
Mn	9.2 ± 1.0	
Cr	8.2 ± 0.8	
Al	7.8 ± 0.6	

TABLE XII: Abundance Ratios of Ionic Species for Pure Elements (with Tantalum Disc)

Element	N^+/N^{++}
Zn	19 ± 2
Cu	8 ± 2
Ni	7 ± 2
Ag	10 ± 2
Mg	5.2 ± 1.0
Co	9 ± 2
Nb	7 ± 2

(4200°C and $>$ 4100°C, respectively) are <u>much</u> higher than the elements under study guarantees that their presence has little effect on the temperature of the spark which is primarily determined by the more volatile constituents.

The data appearing in Tables XI and XII are of interest as the first quantative measurements of their type. Further reference will be made in Chapter III to the copper data where they will be used to make an estimate of the temperature of the spark.

Peak Voltage Effect

The ionization efficiency ratio, Cu^+/Ni^+, was measured with three different peak voltages across the electrodes. The accompanying diagram of the Tesla circuit will be helpful in illustrating these experiments.

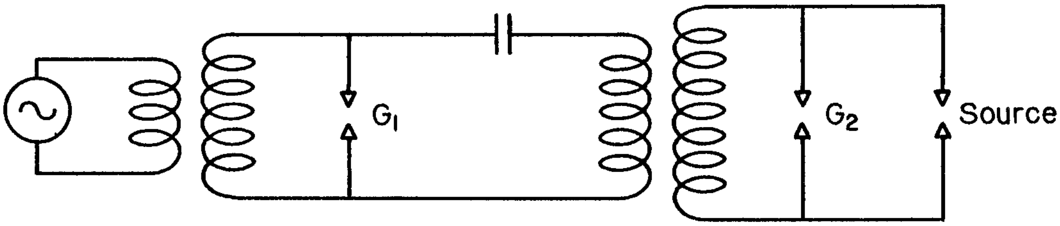

Figure II

Schematic Diagram of Tesla Circuit

In all of the experiments, except those reported in this section, the spark gap G_2 was present in the circuit. The purpose of this narrow gap was to provide a partial shunt to prevent corona discharges (and the accompanying electrical noise) from occurring when the source spark was poor or had stopped.

To study the peak voltage effect, the experiments were carried out a) with G_2 in the circuit, b) with G_2 removed and G_1 adjusted to 2.5 mm and c) with G_2 removed and G_1 adjusted to 4 mm. Thus, three distinctly different peak voltages were applied to the electrodes, representing a variation of at least a factor of three. The results obtained with alloy 712A are shown in Table XIII.

TABLE XIII: $\xi^{+} = Cu^{+}/Ni^{+}$ for Various Peak Voltages

G_2 in circuit	$G_1 = 2.5$ mm G_2 out	$G_1 = 4$ mm G_2 out
1.14 ± 0.02	1.19 ± 0.03	1.16 ± 0.03

Similar experiments were carried out with a pure copper sample. In this case the ratios of the ionic species were measured with the same three peak voltages. Since the ions Cu^{+}, Cu^{++} and Cu^{+++} are spread over a large range of magnetic field and the time needed to scan them is of the order of several minutes and, also, because it is difficult to maintain a steady spark over a long period, the sparking conditions may not have been uniform through the entire time needed to record the +, ++ and +++ ions. This is probably the cause of the considerably larger errors that are associated with the values of the +/++ and +/+++ current ratios shown in Table XIV.

As can be seen from Tables XIII and XIV, within the limits of accuracy of our experiment, we could detect no change with peak voltage either in the ionization efficiency ratio Cu^{+}/Ni^{+} or in the abundance ratios of singly- to multiply-charged ions of copper. This result is of considerable practical importance in the mass spectroscopic analysis of solids in that it indicates that systematic differences are unlikely to arise because of the use of different spark voltages in different laboratories. It is in accord with the belief expressed by Mandelstam (1959) that the potential drop across the spark falls rapidly after breakdown and has a value less than 100 V for most of the discharge. If this is true, the actual voltage at breakdown would have a negligible effect.

TABLE XIV: Peak Voltage Effect on Production of Multiply-Charged Ions of Copper (All Current Ratios)

Gap	Cu^+/Cu^{++}	Cu^+/Cu^{+++}
G_2 in circuit	4.5 ± 0.4	11 ± 1.4
G_1 = 2.5 mm G_2 out	5.0 ± 0.5	12.9 ± 1.0
G_1 = 4 mm G_2 out	4.7 ± 0.8	12.7 ± 1.0

Relative Contributions from Rod and Disc Electrodes

A series of experiments was performed to ascertain the relative numbers of ions that originate from the disc and rod electrodes. Spectra were taken with a certain combination of rod and disc, and then with the rod and disc materials interchanged. The results of these experiments are shown in Table XV where the symbol Fe/Ni refers to the apparent ionization efficiency of iron relative to nickel, Fe^+/Ni^+, calculated as

TABLE XV: Data Relating to the Relative Contributions from Rod and Disc Electrodes

Disc	Rod	Apparent Ionization Efficiency Ratio
Iron	Nickel	Fe/Ni ~0.5
Nickel	Iron	Fe/Ni ~1.6
Copper	Iron	Fe/Cu ~1.5
Iron	Copper	Fe/Cu ~0.2
Nickel	Copper	Cu/Ni ~2.5
Copper	Nickel	Cu/Ni ~0.4

if each electrode were 50% iron and 50% nickel. In actual fact, of course, one electrode is 100% iron and the other is 100% nickel.

Let us assume the rod electrode is f times more efficient than the disc in providing ions for the ion beam. Then, to take the first entry in Table XV as an example, the apparent efficiency ratio Fe/Ni will be 1/f times the actual ratio for identical iron and nickel electrodes. Likewise, the apparent ratio in the second entry will be f times the actual ratio. The values of f deduced by the three combinations shown in Table XV are $f \sim \sqrt{1.6/0.5} \sim 1.8$, $f \sim \sqrt{1.5/0.2} \sim 2.7$ and $f \sim \sqrt{2.5/0.4} \sim 2.5$, respectively. Thus, the rod electrode is apparently ~ 2.5 times more efficient than the disc in contributing ions to the beam.

In addition to the above effect, the disc eventually becomes contaminated with material from the rod electrode, and with some materials this may happen rapidly. As a result there is a further enhancement in the mass spectrum of the elements comprising the rod. Indeed, because of this effect, the value for the factor f, which is given above, may be somewhat in error.

CHAPTER III: TEMPERATURE OF THE VACUUM SPARK

It is well known from both optical and mass spectroscopy that the vacuum spark produces a concentrated, high temperature plasma which is rich in multiply-charged ions. For example, the optical spectra of Fe XVII and Al XII have been observed (Lebedev et al, 1960), and the writer has seen mass spectra photographed by Professor Duckworth in which the W^{+6} spectrum is clearly visible.

The temperature of the vacuum spark has been the subject of two recent experimental investigations in Russia (Akimov and Malkov, 1959 and Lebedev et al, 1960), both presumably prompted by a general interest in controlled thermonuclear reactions. These investigations assume the existence of thermal equilibrium in the spark, an assumption that appears justified on the basis of the calculation by Mandelstam (1959) that the free electron density is $\sim 10^{17}$ per cm^3. This is two orders of magnitude greater than for the arc, where the existence of thermal equilibrium is apparently well established, and allows one to use the Boltzmann equation to calculate the relative populations of the various energy levels.

In the experiments of Akimov and Malkov, the spark temperature was determined by measuring the relative intensities of the spectral lines in the Al III spectrum. The temperature thus found was $\sim 50{,}000^{\circ}K$ but the authors add: " These results must be interpreted as the temperatures of the Al III ions at the instant of excitation. Due to the oscillating nature of the discharge .... it is difficult to say whether these are maximum temperatures or not."

Lebedev et al estimated the spark temperature to be ~200,000°K by observing the intensities of the Al VII lines in the soft x-ray region. They suggested that the lower temperature observed by Akimov and Malkov "characterizes the peripheral (colder) portions or later stages of the discharge." They also demonstrated that the intensity of radiation is applicable for several microseconds after the discharge occurs, albeit decreasing.

Our measurements of the relative numbers of singly-, doubly- and triply-charged ions of copper emerging from the spark provide direct information concerning the population distribution, and can be used to make an independent calculation of the spark temperature, as will now be done.

Calculation of the Spark Temperature, Assuming it to be Constant During the Discharge

Let us recall the ratios of singly- to multiply-charged copper ions given in Chapter II, Table XI:

$$\frac{N^{+}}{N^{++}} = 9.0 \pm 0.8 \qquad \frac{N^{+}}{N^{+++}} = 33 \pm 5$$

For a steady spark temperature, these ratios are given by the Boltzmann expression, viz,

$$\frac{N^{+}}{N^{++}} = e^{(E^{++} - E^{+})/kT} = e^{E'/kT} \tag{3-1}$$

and

$$\frac{N^{+}}{N^{+++}} = e^{E''/kT} \tag{3-2}$$

where $E' = E^{++} - E^{+}$, $E'' = E^{+++} - E^{+}$, and E^{+}, E^{++} and E^{+++} are the energies needed to remove one, two and three electrons, respectively, from an atom of copper. Thus, E^{+} is the first ionization potential (7.68 eV), E^{++} is the sum of the first and second (7.68 + 20.34 = 28.02 eV), and E^{+++} is the sum of the first three (7.68 + 20.34 + 29.3 = 57.32 eV).

The temperature calculated on the basis of $N^{+}/N^{++} = 9.0 \pm 0.8$ is ~100,000°K. Using this spark temperature, we may then compute a value for the corresponding N^{+}/N^{+++} ratio. The value so computed is 330, in poor agreement with the observed value of 33 ± 5, which obviously corresponds to a higher steady temperature than 100,000°K.

This discrepancy may be explicable by assuming, in keeping with the observations of Lebedev et al, that the spark temperature is not constant, and that the highly-ionized species are produced primarily during the early, hottest, period of the discharge. This possibility is investigated in the following section.

Calculation of the Maximum Spark Temperature, T_0, Assuming a Steady Cooling of the Spark

For simplicity, let us assume that the temperature of the spark decreases steadily from an initial maximum value, T_0, according to the relationship

$$T = T_0 - Kt \tag{3-3}$$

where T is the instantaneous temperature, t is the time and K is the constant. This is probably a fair approximation, and should enable us to discover if the observed N^{+}/N^{++} and N^{+}/N^{+++} ratios are explicable in terms of a spark whose temperature declines during each discharge.

The Boltzmann expression for the concentration of singly-charged ions thus becomes

$$n^+ = n_o e^{-E^+/k(T_o - Kt)} \qquad (3\text{-}4)$$

and the total of such ions produced during the period of the discharge is

$$N^+ = \int_{t=0}^{t=T_o/K} n^+ dt = n_o \int_{t=0}^{t=T_o/K} e^{-E^+/k(T_o - Kt)} dt \qquad (3\text{-}5)$$

The integral appearing in equation (3-5) can be evaluated by plotting the integrand (n^+/n_o) as a function of t, and measuring the area under the curve. Figure 12 shows such a plot made for the value $T_o = 160,000^oK$. Also, shown in the Figure are the corresponding plots for n^{++}/n_o and n^{+++}/n_o. Thus, we obtain

$$\frac{N^+}{N^{++}} = \frac{\text{area under } n^+/n_o \text{ curve}}{\text{area under } n^{++}/n_o \text{ curve}} = 8.4 \qquad (3\text{-}6)$$

and $$\frac{N^+}{N^{+++}} = \frac{\text{area under } n^+/n_o \text{ curve}}{\text{area under } n^{+++}/n_o \text{ curve}} = 91 \qquad (3\text{-}7)$$

The corresponding calculated values for $T_o = 2 \times 10^5\ ^oK$ are $N^+/N^{++} = 5.9$ and $N^+/N^{+++} = 53$. The corresponding experimental values, it will be recalled, are 9.0 ± 0.8 and 33 ± 5, respectively. The agreement between these and the calculated values is surprisingly good in the light of the arbitrary assumption which was made concerning the rate of cooling of the spark. To obtain better agreement, one could assume a functional relationship between temperature and time of the form

$$T = f(t) \qquad (3\text{-}8)$$

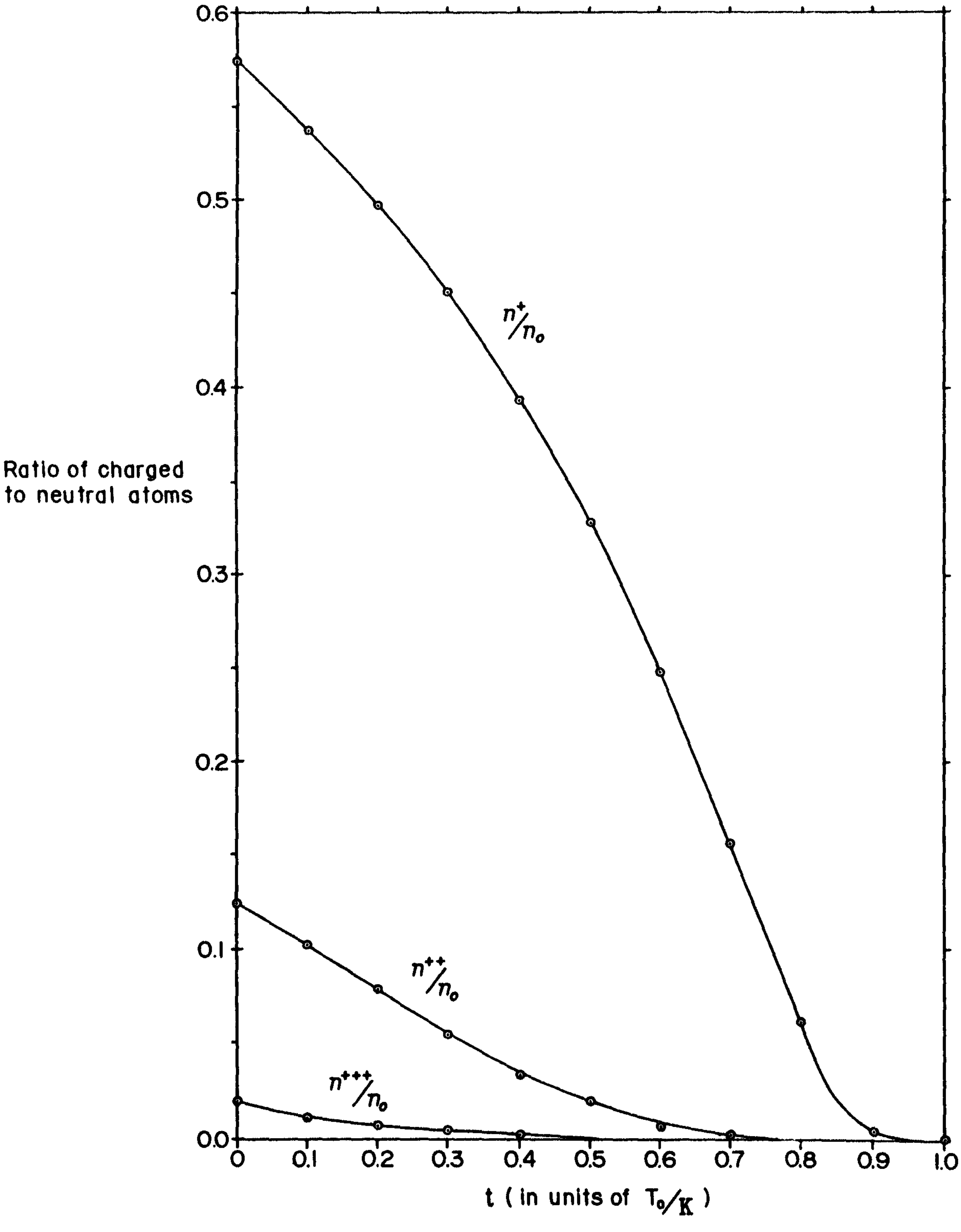
0.6
0.5
0.4
0.3
0.2
0.1
0.0
Ratio of charged to neutral atoms
n^+/n_0
n^{++}/n_0
n^{+++}/n_0
0
0.1
0.2
0.3
0.4
0.5
0.6
0.7
0.8
0.9
1.0
t (in units of T_0/K)

Figure 12

such that

$$9 = \int_0^{t'} e^{(E_2 - E_1)/kT} \, dt = \int_0^{t'} e^{(E_2 - E_1)/kf(t)} \, dt \qquad (3\text{-}9)$$

and

$$33 = \int_0^{t'} e^{(E_3 - E_1)/kT} \, dt = \int_0^{t'} e^{(E_3 - E_1)/kf(t)} \, dt \qquad (3\text{-}10)$$

where t' is the time at which the temperature of the spark has dropped to zero. We have not felt that the precision of our results warrants the labor involved in the exact solution of the simultaneous equations (3-9) and (3-10). We have, however, tried a couple of simple functions and find that it is not hard to improve the concordance between experiment and calculations. These attempts indicate that our data correspond to a maximum spark temperature of

$$T_0 = (1.8 \pm 0.2) \times 10^5 \text{ degrees Kelvin}$$

in good agreement with the result of Lebedev et al (1960) quoted earlier.

CHAPTER IV: ASSOCIATION OF CARBON ATOMS FROM GRAPHITE IN A HIGH FREQUENCY SPARK

Mattauch, Ewald et al reported as early as 1942-43 that graphite electrodes in a high frequency spark produce complex mass spectra of carbon atoms. Ten years later Chupka and Inghram (1953) and R. E. Honig (1953) observed large carbon 'molecules' of the type C_n, emitted from heated graphite (or carbon) filaments. The material emitted from the filament was ionized by electron bombardment and examined in a mass spectrometer. R. E. Honig observed especially large densities of C_3 molecules. In 1959 Pitzer and Clementi developed a molecular orbital theory to predict the properties of carbon vapour. One of their interesting findings was that " the odd species have closed shell structures and lower energies than the even species but that the even species should show greater electron affinity. Both of these results are consistent with the mass spectrometric results of Honig and of Chupka and Inghram." Pitzer and Clementi (1959) also pointed out that, even at a temperature of 2000°K, C_5 molecules will be the most abundant species in the saturated vapour, and at about 2500-3000°K the C_7 species will become comparably abundant. It is not yet known whether the Pitzer and Clementi theory of carbon vapour should also apply in the case of high frequency spark ion source. If it does, because of the much higher temperature in the spark, it would predict the formation of even larger molecular carbon ions. Such an effect was observed by Dörnenburg and Hintenberger (1959, 1961) using a spark ion source. They found molecular carbon ions as high as C_{28}^+. Shortly thereafter Baun and Fischer (1961) also observed very large molecular carbon ions from graphite electrodes. It is interesting to note that the largest molecule observed by both groups was C_{28}. Both groups present their data in the form of plots of the intensity of C_n^+ ions versus C_n, and both curves show roughly similar periodic variations of intensity. But the two curves differ in certain significant respects, the most important difference relating to the abundance of C_2^+ ions compared to C_3^+. Baun and Fischer observed (although they did not plot the intensity of C_2^+ and C_3^+ ions) the C_2^+ ions to be more abundant than C_3^+, whereas Dörnenburg and Hintenberger found just the opposite (and showed the result on their intensity plot). This serious discrepancy between the two sets of data prompted us to repeat the relevant portion of the experiment. It should be mentioned here that the two groups of workers differed in the source geometry which they employed and to some extent in their detection system. Dörnenburg and Hintenberger used the geometry of a graphite rod sparking against the wall of a hole in a graphite disc and electrical detection (the technique of charging a condenser and noting the galvanometer deflection when the condenser is discharged) for the fairly intense ions (up to C_{19}^+ ions) and a calibrated photographic method for the less intense, heavier, molecular ions. Baun and Fischer used the two-rod sparking geometry and photographic detection throughout. But the latter gave no information concerning the calibration of photographic plates, nor did they state the potential through which the ions are accelerated. Of the two differences, much the more important one (see below) is that one group employed electrical detection for the C_2^+ and C_3^+ ions whereas the other employed photographic plates. The present experiment used the rod-disc geometry, similar to that of Dörnenburg and Hintenberger, with vibrating reed electrometers for ion detection (ratio measuring system as described earlier). Only C_1^+, C_2^+, C_3^+ and some C_5^+ ions were detected. The only point of interest at present is to check the C_3^+/C_2^+ ratio. Our datum is compared below with that of Dörnenburg and Hintenberger.

TABLE XVI: C_3^+/C_2^+ Intensity Ratio

Ratio	This Work	Dörnenburg and Hintenberger (1959,1961)
C_3^+/C_2^+	2.6 ± 0.2	2.89

Although the error is not given for the Dörnenburg and Hintenberger result, it is at least large enough to cause the two values to overlap. Clearly, our value substantiates their result.

One might speculate concerning the cause of the Baun and Fischer results. It is entirely possible that they used a correct mass-versus-intensity curve for calibrating their photographic plates, but overlooked the fact that C_n dissociates on striking the plate into nC. This oversight could sabotage the interpretation of their results.

We have done a few experiments with the two-electrode system used by Baun and Fischer -- sufficient to demonstrate that the discrepancy is not caused by the geometry of the source.

CHAPTER V: THE Ni^{58}/Ni^{60} AND Cu^{63}/Cu^{65} ABUNDANCE RATIOS

Many of the mass spectra obtained in the course of the work described in Chapter II were suitable for calculating the natural isotopic abundance ratios Ni^{58}/Ni^{60} and Cu^{63}/Cu^{65}. The values that were obtained therefrom will now be discussed in relation to existing values for these ratios.

The Ni^{58}/Ni^{60} Natural Abundance Ratio

The isotopic constitution of nickel was first studied by F. W. Aston (1923, 1935), using as a source of ions an electric discharge in a vapour of nickel carbonyl, $Ni(CO_4)_4$. His value for the Ni^{58}/Ni^{60} ratio is shown in Table XVII, together with the values which have been obtained in subsequent investigations.

On a large number of the mass spectra obtained with a nickel-copper alloy as the rod electrode either the peaks corresponding to Ni^{58} and/or Cu^{63} were off-scale or those corresponding to Ni^{60} and/or Cu^{65} were too low for accurate measurement. From the remainder we have selected those for which the measured Ni^{58}/Ni^{60} ratio lies in the range 2.59 ± 0.30 and the measured Cu^{63}/Cu^{65} ratio lies in the range 2.22 ± 0.30 (the accepted value of the Cu^{63}/Cu^{65} ratio is close to 2.22 -- see next section). We have 104 such spectra, and they exhibit a satisfactory Gaussian distribution with mean value 2.58 ± 0.03. We have obtained a second, independent, value from spectra got with pure nickel as the rod electrode. We have 124 such spectra and they yield a mean value 2.56 ± 0.08.

TABLE XVII: Existing Values for the Ni^{58}/Ni^{60} Abundance Ratio

Investigator	Type of Source	Type of Detector	Ni^{58}/Ni^{60} Ratio
Aston (1935)	Discharge in $Ni(CO_4)_4$	Photographic plate	2.50 ± ?
Straus (1941)	Spark	Electrical	2.13 ± ?
Valley (1941)	Electron bombardment of Ni vapour	Electrical	2.52 ± ?
Ewald (1944b)	Discharge in $Ni(CO_4)_4$	Photographic plate	2.68 ± 0.06
Inghram and Hess (1948)	Electron bombardment of ?	Electrical	2.59 ± ?
White and Cameron (1948)	Electron bombardment of $NiCl_2$	Electrical	2.59 ± 0.07
Mattraw and Pachucki (1952)	Electron bombardment of ?	Electrical	2.59 ± ?

In this way, by combining the two independent values for the Ni^{58}/Ni^{60} ratio, we obtain the overall mean value

$$Ni^{58}/Ni^{60} = 2.58 \pm 0.03.$$

This value is consistent with the currently-accepted one and is apparently the most accurate value to date.

The probable errors stated above represent the statistical consistency of the data. To this error should be added, of course, the error associated with the detecting and recording systems. It will be shown in a subsequent section, however, that this latter error makes no significant contribution to the total error. Hence, the value for the Ni^{58}/Ni^{60} ratio given above is our final value.

The Cu^{63}/Cu^{65} Natural Abundance Ratio

Cu^{63} and Cu^{65} are the only naturally-occurring isotopes of copper. Their existence was established by Aston in 1924, who also reported that their abundances were approximately in the ratio 5:2. This result and others obtained later are shown in Table XVIII.

As for the Ni^{58}/Ni^{60} ratio, we have two independent values for the Cu^{63}/Cu^{65} ratio -- the first obtained from spectra for which the observed nickel ratios lie in the range 2.59 ± 0.30 <u>and</u> the observed copper ratios in the range 2.22 ± 0.30, and the second from spectra obtained with pure copper as the rod electrode. The two values are 2.21 ± 0.02 and 2.24 ± 0.07, respectively, giving the overall mean value

$$Cu^{63}/Cu^{65} = 2.21 \pm 0.02.$$

This result is consistent with existing values but is not so accurate as the one (2.24 ± 0.01) reported by Hess, Inghram and Hayden in 1948.

TABLE XVIII: Existing Values for the Cu^{63}/Cu^{65} Abundance Ratio

Investigator	Type of Source	Type of Detector	Cu^{63}/Cu^{65} Ratio
Aston (1924)	CuCl anode in a discharge	Photographic plate	2.5 ± ?
Ewald (1944a)	Spark	Photographic plate	2.33 ± 0.02_4
Dempster (1946)	Spark	Electrical	2.23 ± 0.03
Dempster (1946)	Spark	Photographic plate	2.35 ± 0.02
Duckworth and Hogg (1947)	Spark	Photographic plate	2.28 ± 0.01_3
Brown and Inghram (1947)	Electron bombardment of CuCl, $CuCl_2$	Electrical	2.24 ± ?
White and Cameron (1948)	Electron bombardment of CuCl	Electrical	2.22 ± 0.02
Hess, Inghram and Hayden (1948)	Electron bombardment of ?	Electrical	2.235 ± 0.010
Hibbs (1950)	Electron bombardment of ?	Electrical	2.22 ± ?

It has the merit, however, that the type of source (spark) and the type of detector (simple Faraday cup with linear amplifier) guarantee that mass discrimination is at a minimum. For this reason, the confirmation of the correctness of existing values is of some worth.

Calibration of the Detection Systems

The calibration of the combined detection and recording systems was carried out in the following way. With switch S_1 closed (see Figure 13), S_2 was alternately switched between A and B. That is, voltages V_1 and V_2 were alternately applied to the input of the vibrating reed electrometer and the output voltages were recorded on the chart paper of the recorder. In the circuit diagram, R_1 and R_2 were precision resistors ($R_1 = 1000\Omega$ and $R_2 = 1200\,\Omega$).

We have

$$V_1 = IR_1$$

$$V_2 = I(R_1 + R_2)$$

$$\therefore \frac{V_2}{V_1} = \frac{R_2 + R_1}{R_1}$$

$$= \frac{1201.94 + 998.79}{998.79}$$

$$= 2.204 \pm 0.006$$

where the numeral values given for R_1 and R_2 are those obtained with a precision bridge (accuracy 0.02%).

If the combined detector-plus-recorder system is linear, the above ratio should be equal to the ratio y/x, where y and x are the recorder readings (as taken from the chart paper) for the two cases. Both the isotopic current and monitor systems were subjected to this test, with the following results:

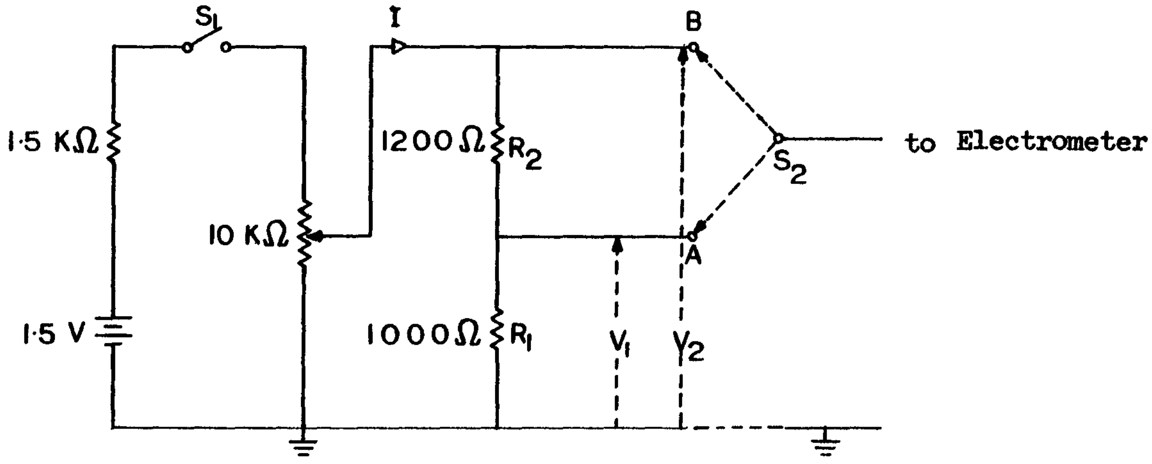

Fig. 13

Circuit for Calibrating Detection Systems

Isotopic current system $(R_2+R_1)/R_1 = 2.202 \pm 0.006$ $y/x = 2.20 \pm 0.01$

Monitor system $(R_2+R_1)/R_1 = 2.202 \pm 0.006$ $y/x = 2.22 \pm 0.04$

In these tests the current through R_1 and R_2 was varied in order to check the linearity at various signal levels. The values shown for y/x are averages of the several such cases.

It can be seen that the isotopic current system is linear to such an extent that the accuracy of the isotopic ratio values is not limited on this account. For the monitor system the linearity is not so good but, on the other hand, small departures from linearity are not so important. If the monitor current were completely steady, the linearity of the monitor system would be a matter of indifference. As it is, the monitor current fluctuates -- but not a great deal during the time taken to move from one isotope to the next. Under these circumstances the fact that the monitor system is non-linear to 2% has a relatively unimportant effect on the accuracy of the experiment. In a very strict sense, however, it does contribute some error.

REFERENCES

Akimov, E. A. and Malkov, I. P. (1959) Optics and Spectroscopy VI, 56.

Aston, F. W. (1923) Phil. Mag. 45, 936.

Aston, F. W. (1924) Phil. Mag. 47, 395.

Aston, F. W. (1935) Proc. Roy. Soc. A149, 396.

Baun, W. L. and Fischer, D. W. (1961) J. Chem. Phys. 35, 1518.

Brown, H. S. and Inghram, M. G. (1947) Phys. Rev. 72, 347.

Chakravarty, B., Venkatasubramanian, V. S. and Duckworth, H. E. (1962) Advances in Mass Spectrometry, Vol. 2, Pergamon Press, p. 128.

Chupka, W. A. and Inghram, M. G. (1953) J. Chem. Phys. 21, 371.

Chupka, W. A. and Inghram, M. G. (1953) J. Chem. Phys. 21, 1313.

Chupka, W. A. and Inghram, M. G. (1955) J. Phys. Chem. 59, 100.

Craig, R. D., Errock, G. A. and Waldron, J. D. (1959) Advances in Mass Spectrometry, Pergamon Press, p. 136.

Dempster, A. J. (1935) Proc. Amer. Phil. Soc. 75, 755.

Dempster, A. J. (1936) Rev. Sci. Inst. 7, 46.

Dempster, A. J. (1946) U. S. Dept. of Commerce, MDDC, 370.

Dempster, A. J. (1946) Report CP-3445.

Dörnenburg, E. and Hintenberger, H. (1959) Z. Naturforsch. 14a, 765.

Dörnenburg, E. and Hintenberger, H. (1961) Z. Naturforsch. 16a, 532.

Dörnenburg, E. and Hintenberger, H. (1961) Z. Naturforsch. 16a, 535.

Duckworth, H. E. and Hogg, B. G. (1947) Phys. Rev. 71, 212.

Duckworth, H. E. (1950) Rev. Sci. Inst. 21, 54.

Ewald, H. (1944a) Z. Physik 122, 487.

Ewald, H. (1944b) Z. Physik 122, 686.

Gorman, J. G., Jones, E. J. and Hipple, J. A. (1951) Anal. Chem. 23, 438.

Graham, R. L., Harkness, A. L. and Thode, H. G. (1947) J. Sci. Inst. 24, 119.

Hahn, O., Strassmann, F., Mattauch, J. and Ewald, H. (1942) Naturwiss. 30, 541.

Hannay, N. B. and Ahearn, A. J. (1954) Anal. Chem. 26, 1056.

Hess, D. C., Inghram, M. G. and Hayden, R. J. (1948) Phys. Rev. 74, 1531.

Hibbs, R. F. (1950) Y-648, Quoted in Nuclear Data Sheets 58-9 110, Appendix 2-2.

Hipple, J. A. and Gorman, J. G. (1951) Symposium on Chemical Analysis of Solids.

Honig, R. E. (1953) Phys. Rev. 91, 465.

Honig, R. E. (1954) J. Chem. Phys. 22, 126.

Inghram, M. G. and Hess, D. C. (1948) ANL-4120, Quoted in Nuclear Data Sheets 58-9 110, Appendix 2-2.

Lebedev, S. V., Mandel'shtam, S. L. and Rodin, G. M. (1960) Soviet Physics JETP 37, 248.

Mandelstam, S. (1959) Spectrochemica Acta 15, 255.

Mattauch, J., Ewald, H., Hahn, O. and Strassmann, F. (1943) Z. Phys. 120, 598.

Mattraw, H. C. and Pachucki, C. F. (1952) AECU-1903.

Meek, J. M. and Craggs, J. D. (1953) Electrical Breakdown of Gases, Clarendon Press, Oxford.

Pitzer, K. S. and Clementi, E. (1959) J. Amer. Chem. Soc. 81, 4477.

Robinson, C. F. (1960) Radio Frequency Noise Suppression in the Vacuum Spark, Research Report II-448.

Strauss, H. A. (1941) Phys. Rev. 59, 430.

Valley, G. E. (1941) Phys. Rev. 59, 836.

White, F. A. and Cameron, A. E. (1948) Phys. Rev. 74, 991.